Microphysical and thermodynamic retrievals using polarimetric radars

Alexander Ryzhkov

University of Oklahoma, USA

Layout of the talk

- Microphysical retrievals
- Thermodynamic retrievals
- Some thoughts on forward operators

Two possible ways to optimize microphysical parameterization of NWP models

- Radar microphysical retrievals
- Forward radar operators

Radar microphysical retrievals

Estimation of liquid water content (LWC)

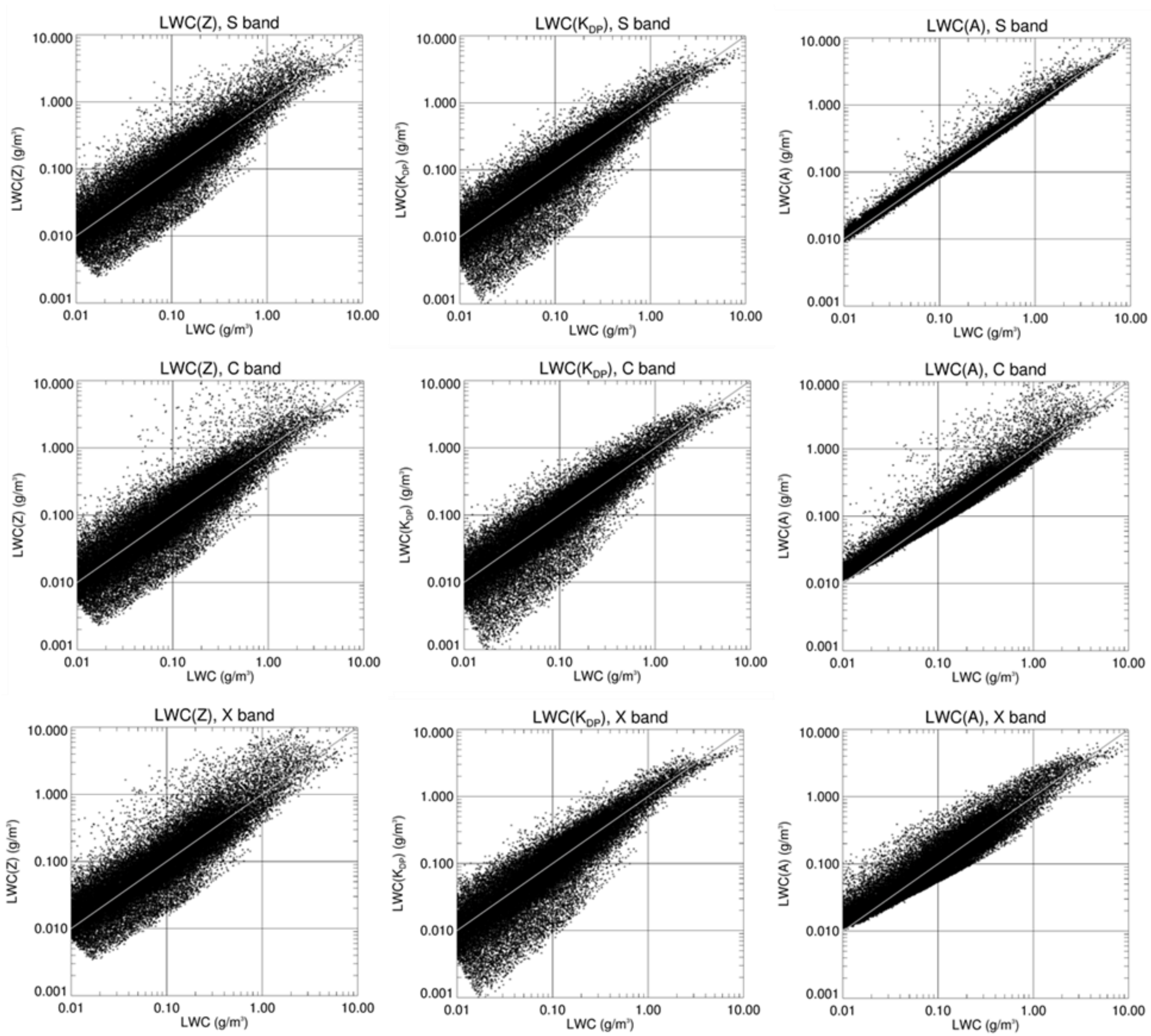

Estimation of median volume diameter of raindrops

S band

$$D_0 = 0.171 Z_{DR}^3 - 0.725 Z_{DR}^2 + 1.48 Z_{DR} + 0.717$$ Brandes et al. (2002) Florida

$$D_0 = 0.0436 Z_{DR}^3 - 0.216 Z_{DR}^2 + 1.08 Z_{DR} + 0.659$$ Cao et al. (2008) Oklahoma

C band

$$\begin{cases} D_0 = 0.0203 Z_{DR}^4 - 0.149 Z_{DR}^3 + 0.221 Z_{DR}^2 + 0.557 Z_{DR} + 0.801 & \text{if } Z_{DR} < 1.25\,\text{dB} \\ D_0 = 0.0355 Z_{DR}^3 - 0.302 Z_{DR}^2 + 1.06 Z_{DR} + 0.684 & \text{if } Z_{DR} > 1.25\,\text{dB} \end{cases}$$ Bringi et al. (2009) Darwin

X band $D_0 = 1.46 Z_{DR}^{0.49}$ Matrosov et al. (2007) California

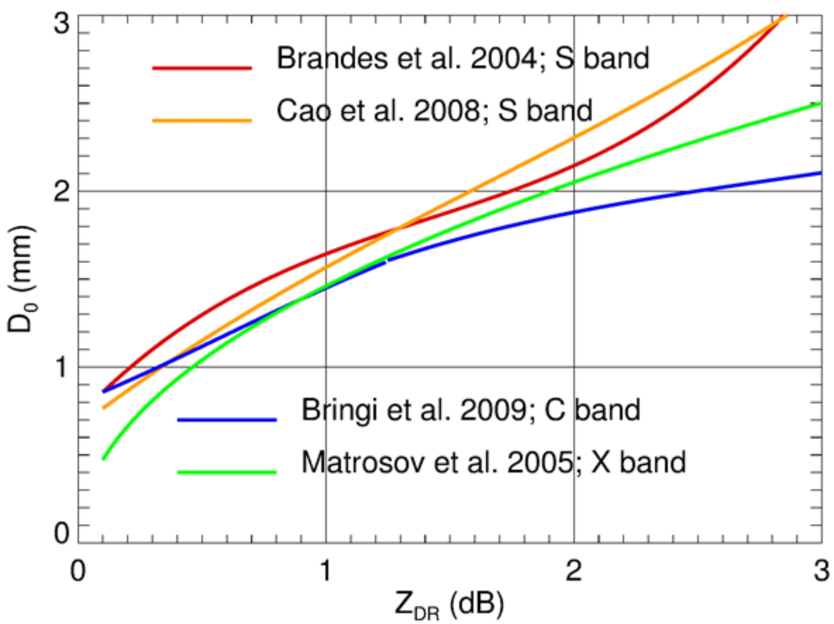

Estimation of normalized concentration N_w

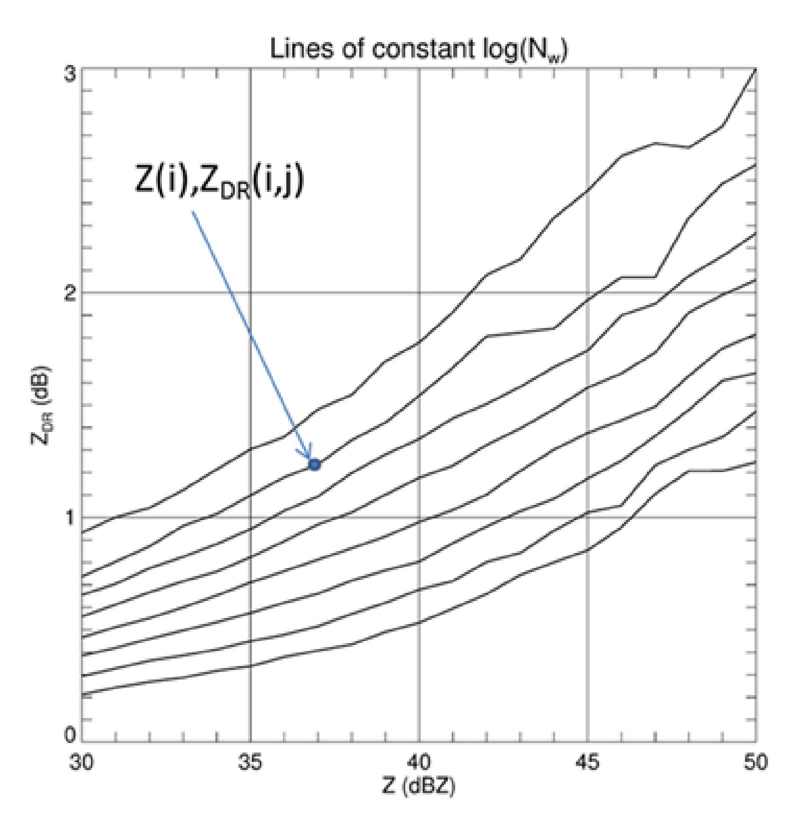

$\text{Log}(N_w)$	$\text{Log}(N_w)$ index
< 2.75	0
2.75 - 3.00	1
3.00 - 3.25	2
3.25 - 3.50	3
3.50 - 3.75	4
3.75 - 4.00	5
4.00 - 4.25	6
> 4.25	7

Spatial distribution of Z, N_w, and D_0 in MCS

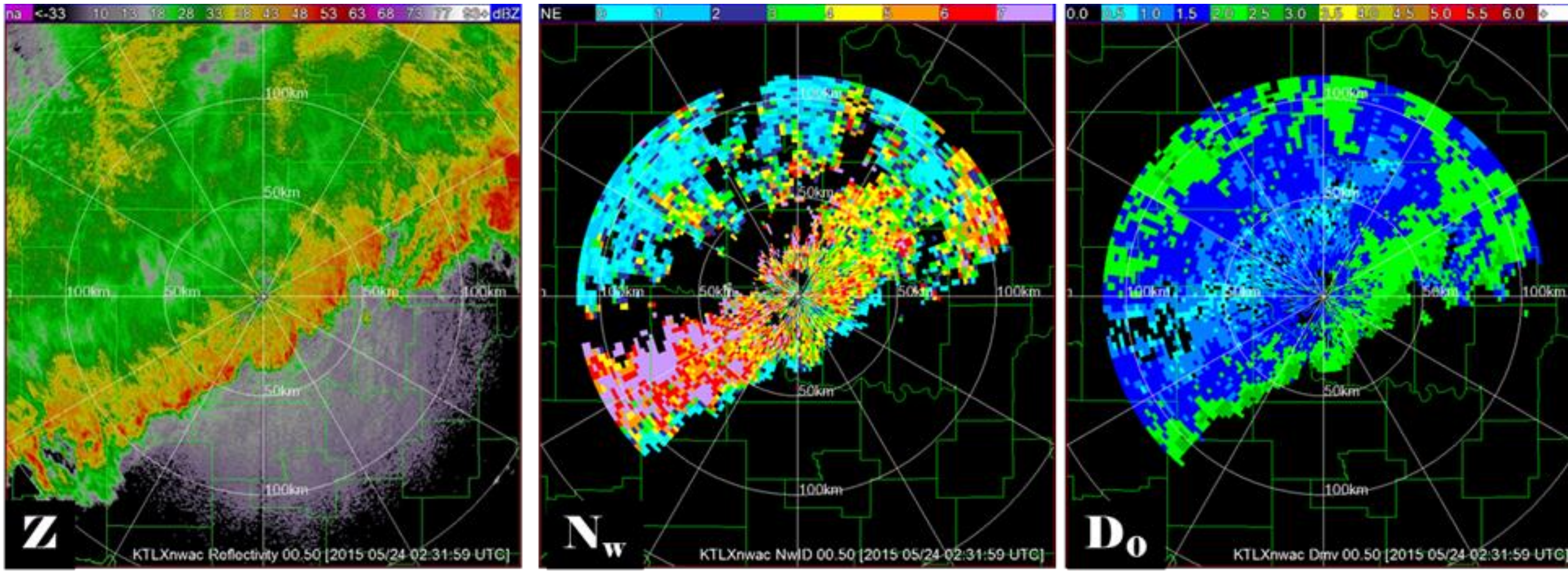

Log(N_w) index	0	1	2	3	4	5	6	7
Log(N_w)	< 2.75	2.75 – 3	3 – 3.25	3.25 – 3.5	3.5 – 3.75	3.75 – 4	4 – 4.25	> 4.25

Ice microphysical retrievals

- **All existing ice microphysical retrievals are based on the use of radar reflectivity Z measured at a single or multiple radar frequencies**

- **The IWC(Z) relations are notoriously inaccurate because they are strongly parameterized by (a) mass-weighted diameter D_m , (b) total concentration N_t , and (c) density (or degree of riming)**

$$N(D) = N_{0s} \exp(-\Lambda_s D) \qquad \rho(D) = \alpha D^{-1} \qquad \Lambda_s = 4 / D_m$$

$$IWC = 3.81 10^{-4} \alpha^{-0.2} N_{0s}^{0.4} Z^{0.6} \qquad IWC = 3.09\, 10^{-3} \frac{Z}{\alpha D_m^2}$$

- D_m varies 2 orders of magnitude
- N_t varies 4 orders of magnitude
- α changes at least by a factor of 4

Dependence of the multiplier in the S(Z) relation on N_{0s} retrieved from the snow disdrometer measurements

Bucovcic et al. 2018

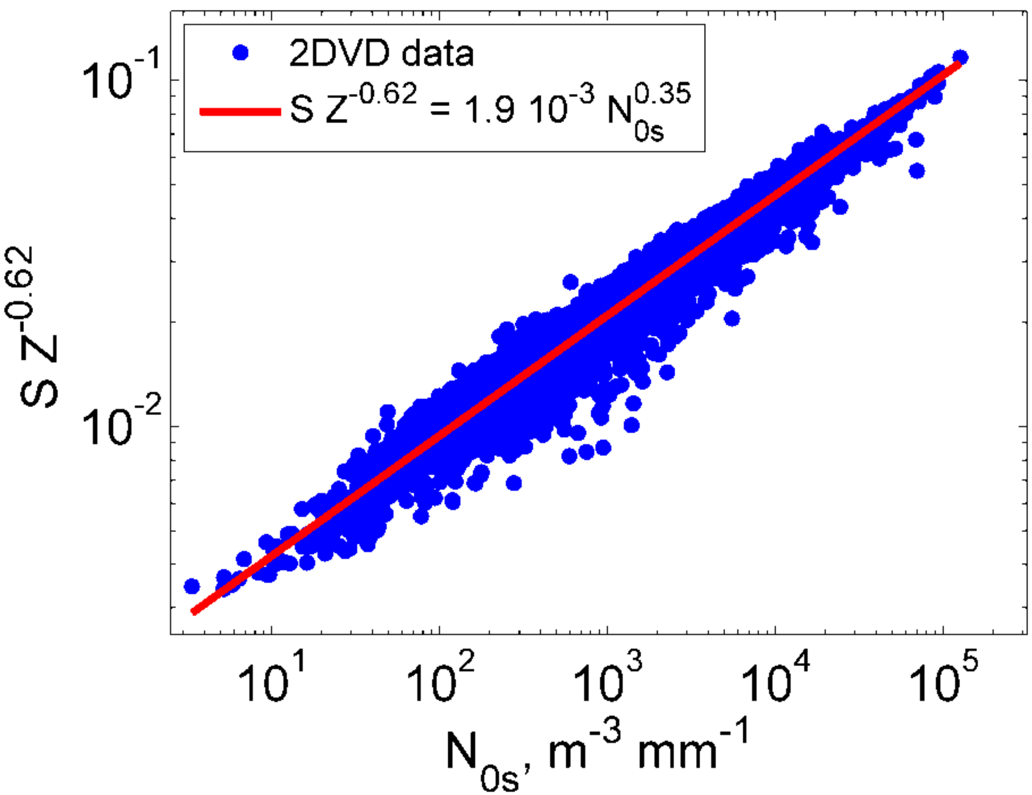

Basic formulas for polarimetric ice retrievals

$$Z = \frac{|K_\mathrm{i}|^2}{|K_\mathrm{w}|^2}\frac{1}{\rho_\mathrm{i}^2}\int \rho_\mathrm{s}^2(D)D^6N(D)dD$$

$$K_\mathrm{DP} = \frac{0.27\pi}{\lambda\rho_i^2}\left(\frac{\varepsilon_\mathrm{i}-1}{\varepsilon_\mathrm{i}+2}\right)^2\int F_{shape}F_{orient}\rho_\mathrm{s}^2(D)D^3N(D)dD$$

Z is proportional to the 4th moment of snow SD whereas K_{DP} is proportional to its 1st moment

Exponential size distribution

$$Z = 5.30\,10^{-3}\alpha^2N_{0\mathrm{s}}D_\mathrm{m}^5$$

$$K_\mathrm{DP} = 1.02\,10^{-2}F_{shape}F_{orient}\frac{\alpha^2N_{0\mathrm{s}}}{\lambda}D_\mathrm{m}^2$$

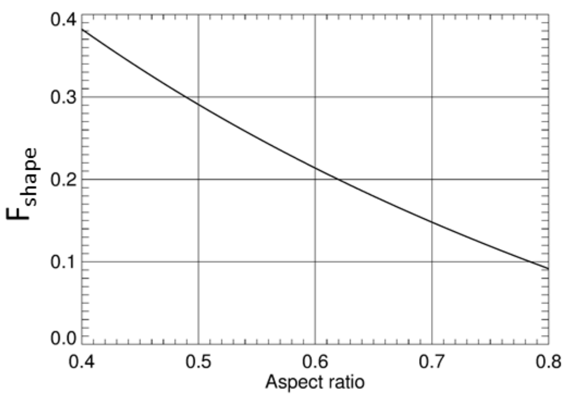

$$\frac{Z}{K_\mathrm{DP}\lambda} = 0.520\frac{D_\mathrm{m}^3}{F_{shape}F_{orient}}$$

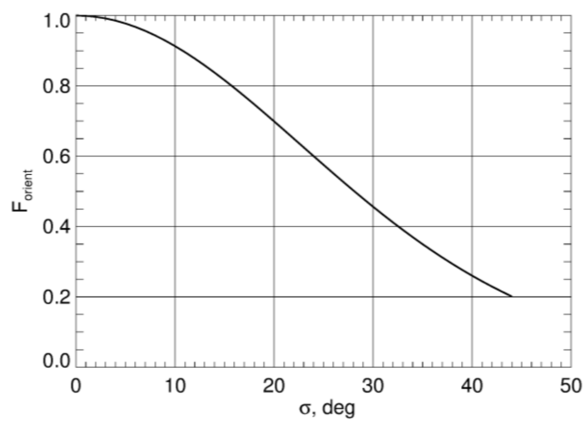

Median volume diameter as a function of $[Z/(K_{DP}\lambda)]^{1/3}$

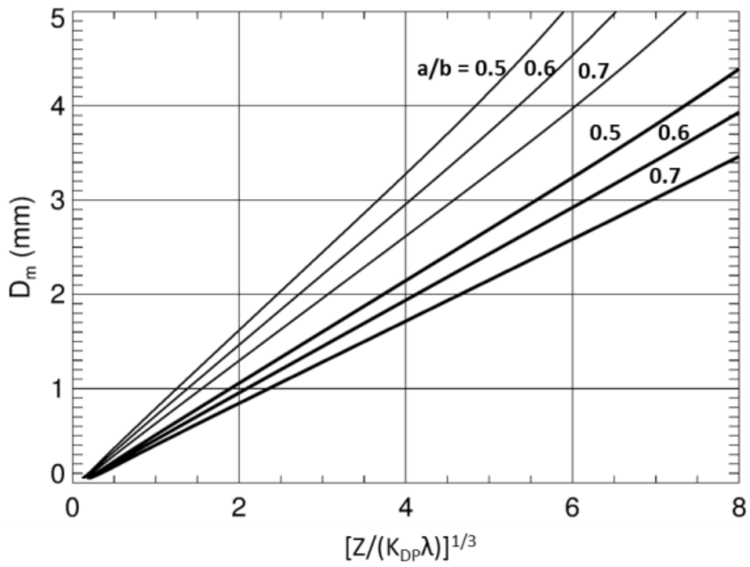

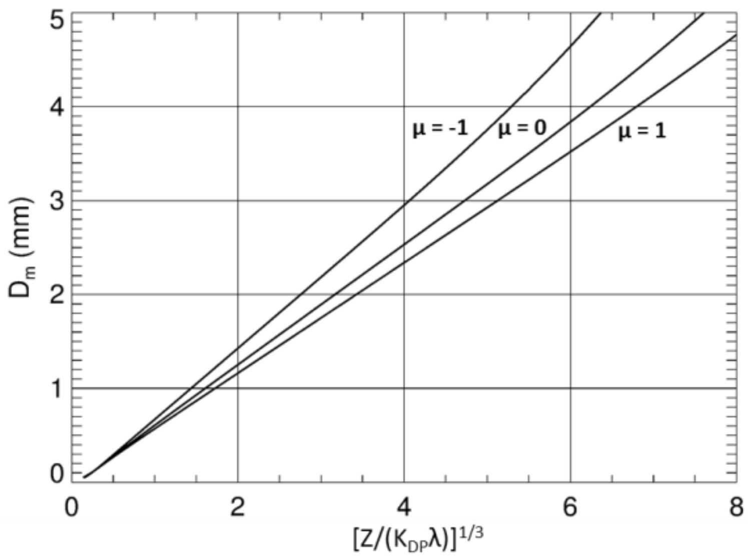

Thin lines – σ = 10^{o}
Thick lines – σ = 40^{o}

$$\sigma = \frac{180}{\pi} \frac{L_{dr}^{1/2}}{(1 + Z_{dr}^{-1} - 2\rho_{hv} Z_{dr}^{-1/2})^{1/2}}$$

The width of the canting angle distribution σ in ice typically varies between 10 and 40^{o}. This is a serious source of uncertainty

Utilization of the Z_{DP}/K_{DP} ratio for estimation of D_m

$$Z_{DP} = Z_h - Z_v$$

$$h = cL^d$$

Crystal habit	c	d
1. Dendrites	0.038	0.377
1. Solid thick plate	0.230	0.778
1. Hexagonal plates	0.047	0.474
1. Solid columns (L/h < 2)	0.637	0.958
1. Solid columns (L/h > 2)	0.308	0.927
1. Hollow columns (L/h < 2)	0.541	0.892
1. Hollow columns (L/h > 2)	0.309	0.930
1. Long solid columns	0.128	0.437
1. Solid bullets (L < 0.3 mm)	0.250	0.786
1. Hollow bullets (L > 0.3 mm)	0.185	0.532
1. Elementary needles	0.073	0.611

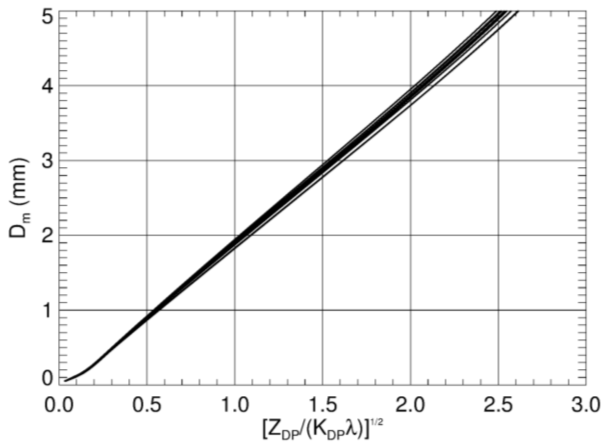

$$D_{\mathrm{m}} = -0.1 + 2.0\,\eta \qquad \eta = \left(\frac{Z_{\mathrm{DP}}}{K_{\mathrm{DP}}\lambda}\right)^{1/2}$$

$$\gamma = \alpha D_m^2 \approx 0.78\eta^2 = 0.78\frac{Z_{DP}}{K_{DP}\lambda}$$

$$\log(N_{\mathrm{t}}) = 0.1Z(\mathrm{dBZ}) - 2\log(\gamma) - 1.33$$

$$IWC \approx 4.010^{-2}\frac{K_{DP}\lambda}{1 - Z_{dr}^{-1}}$$

The Z_{DP}/K_{DP} ratio provides estimate of D_m which is immune to the particles shape and orientation

Midlatitude vs. Tropical MCSs

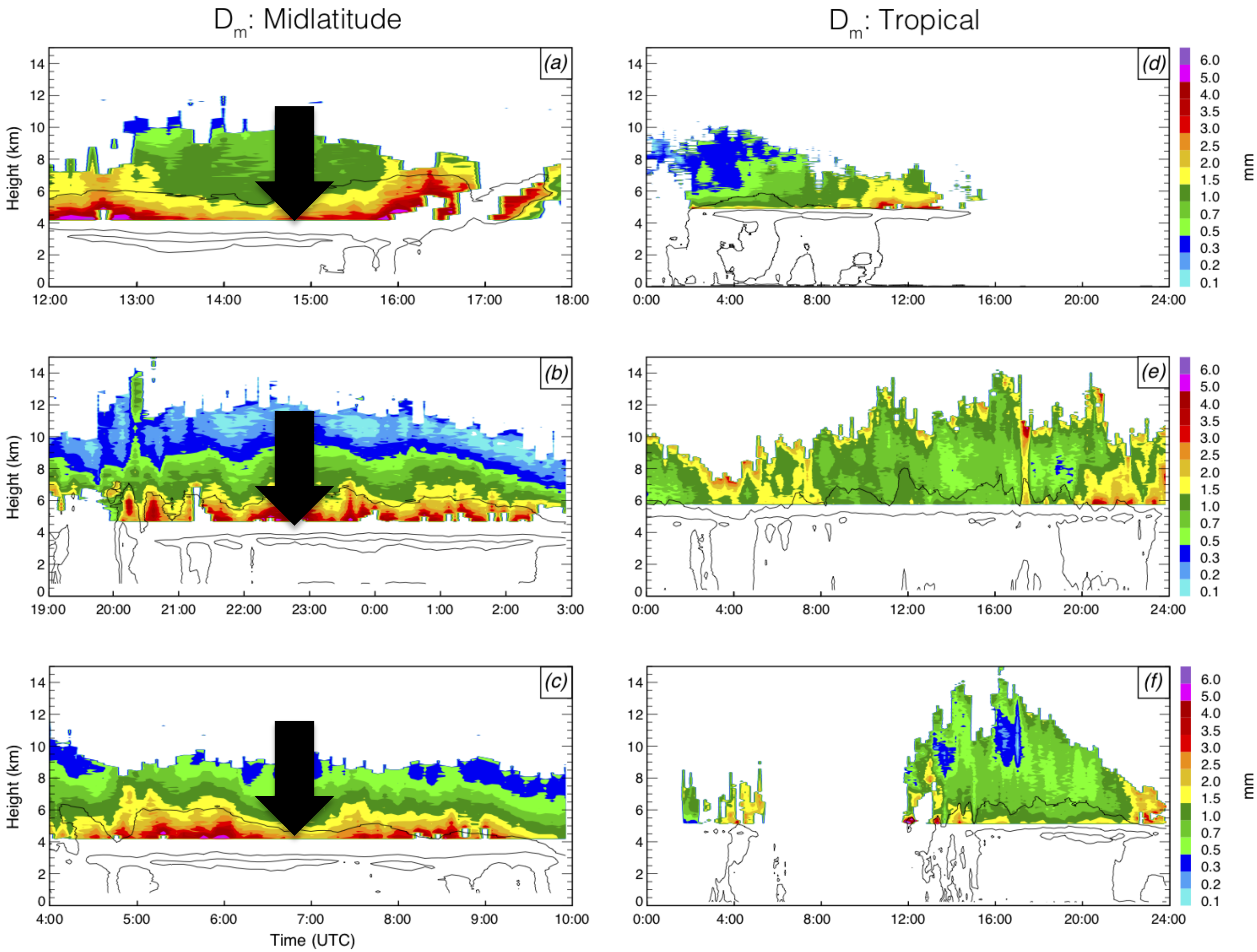

Midlatitude vs. Tropical MCSs

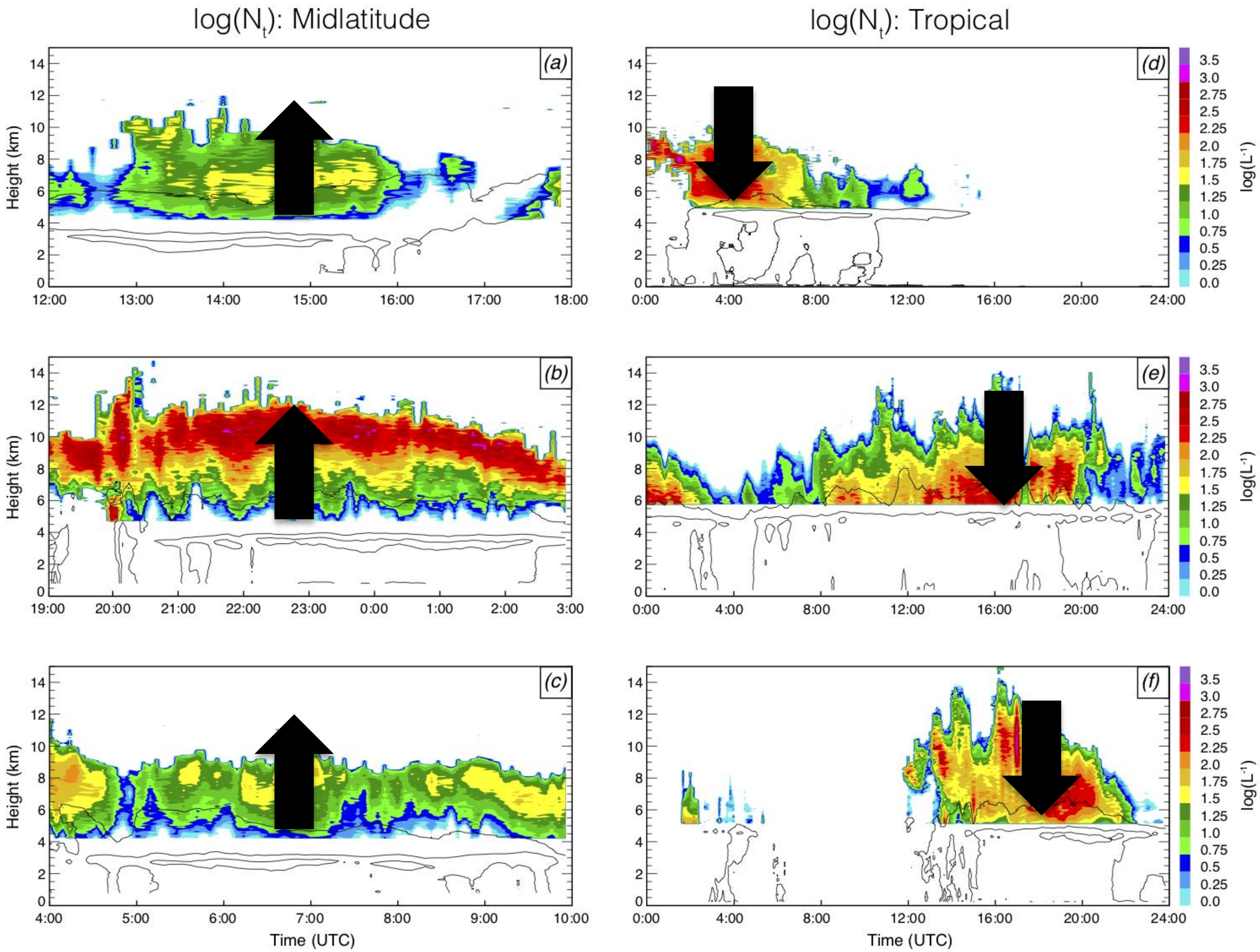

amanda.murphy@ou.edu

Midlatitude vs. Tropical MCSs

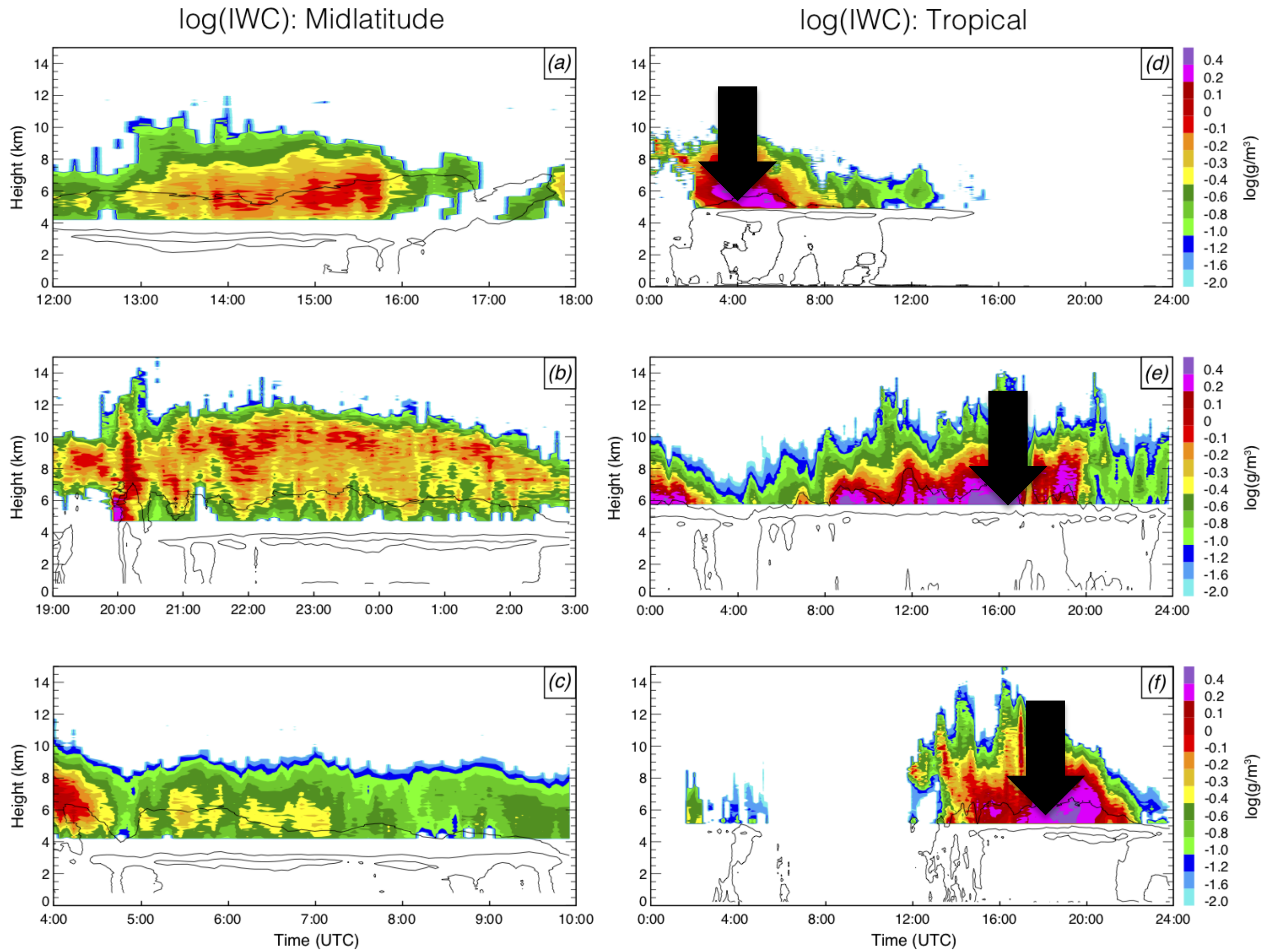

Radar thermodynamic retrievals

Warming / cooling rates retrieved from radar data

10-dBZ height used as an index of lookup tables

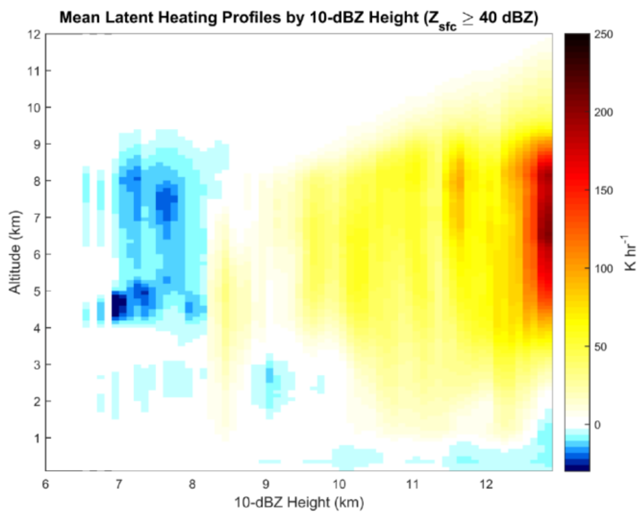

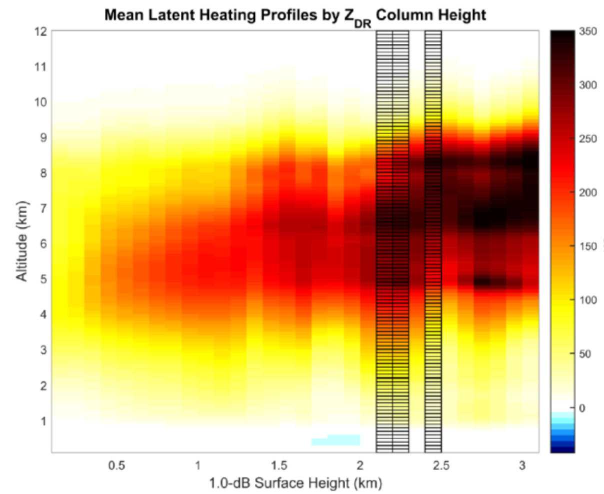

1-dB Z_{DR} column height used as an index of lookup tables

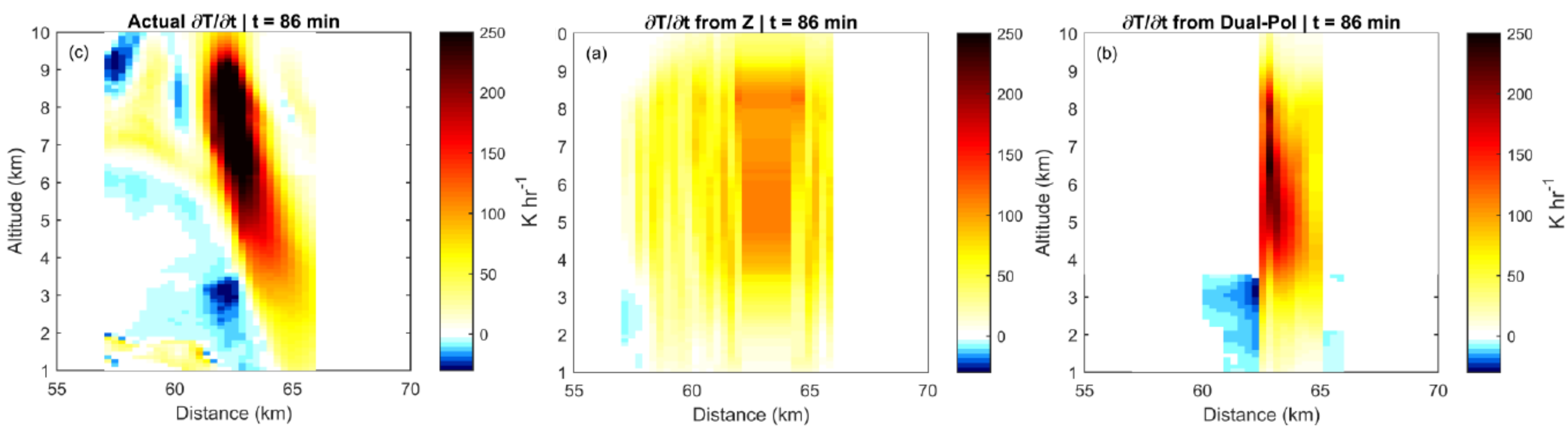

The use of the Z_{DR} column - based index produces much more realistic warming / cooling rates than Z – based index of latent heat profiles

Cooling rates due to evaporation of rain

Xie et al. 2016

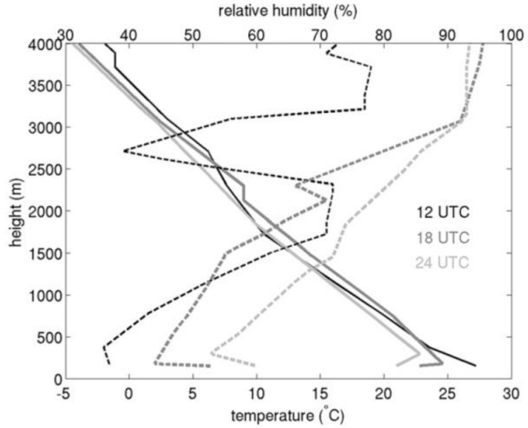

- Evaporation – induced cooling profiles in rain can be derived using a simple 1D evaporation model
- Values of Z and Z_{DR} at the top of the rain layer can be used as indexes of lookup tables for cooling rates
- Depending on Z_{DR}, cooling rates differ by an order of magnitude for the same Z

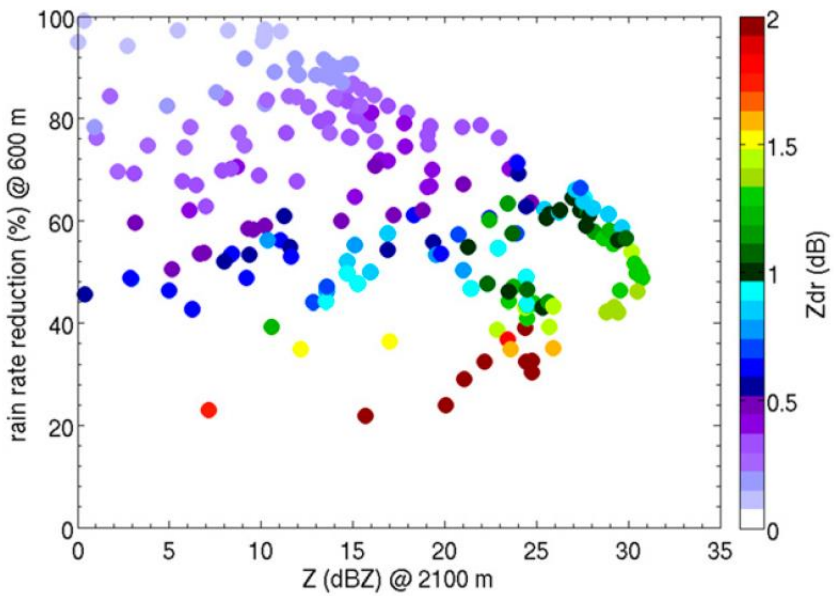

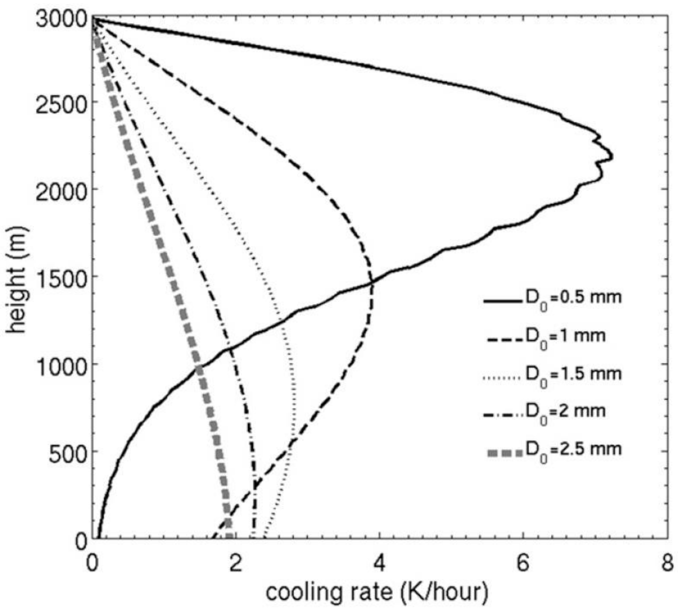

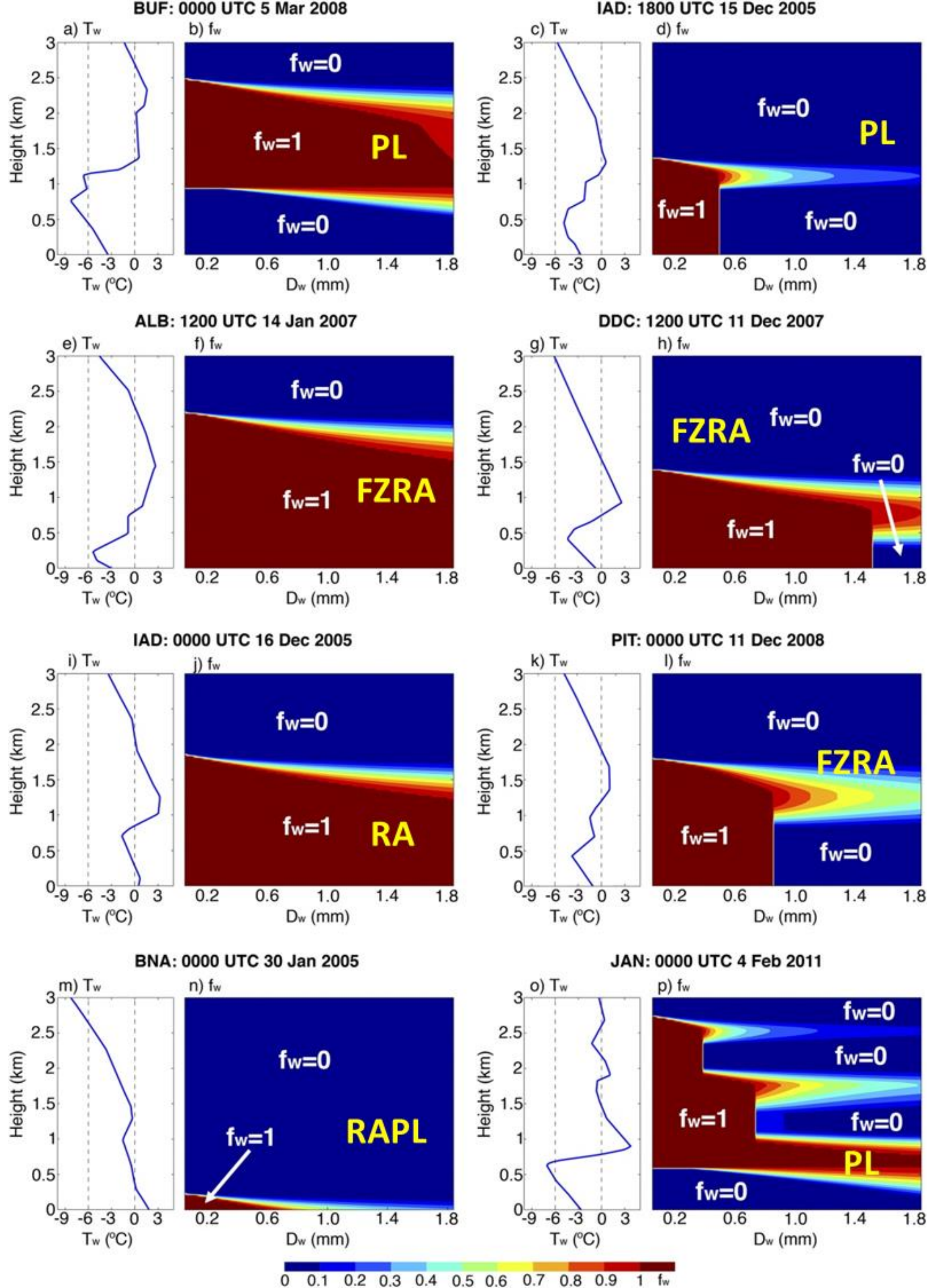
BUF: 0000 UTC 5 Mar 2008
a) Tw
b) fw
fw=0
fw=1
PL
fw=0
IAD: 1800 UTC 15 Dec 2005
c) Tw
d) fw
fw=0
PL
fw=1
fw=0
ALB: 1200 UTC 14 Jan 2007
e) Tw
f) fw
fw=0
fw=1
FZRA
DDC: 1200 UTC 11 Dec 2007
g) Tw
h) fw
FZRA
fw=0
fw=0
fw=1
IAD: 0000 UTC 16 Dec 2005
i) Tw
j) fw
fw=0
fw=1
RA
PIT: 0000 UTC 11 Dec 2008
k) Tw
l) fw
fw=0
FZRA
fw=1
fw=0
BNA: 0000 UTC 30 Jan 2005
m) Tw
n) fw
fw=0
fw=1
RAPL
JAN: 0000 UTC 4 Feb 2011
o) Tw
p) fw
fw=0
fw=0
fw=1
fw=0
PL
fw=0
Height (km)
Tw (ºC)
Dw (mm)
0 0.1 0.2 0.3 0.4 0.5 0.6 0.7 0.8 0.9 1 fw

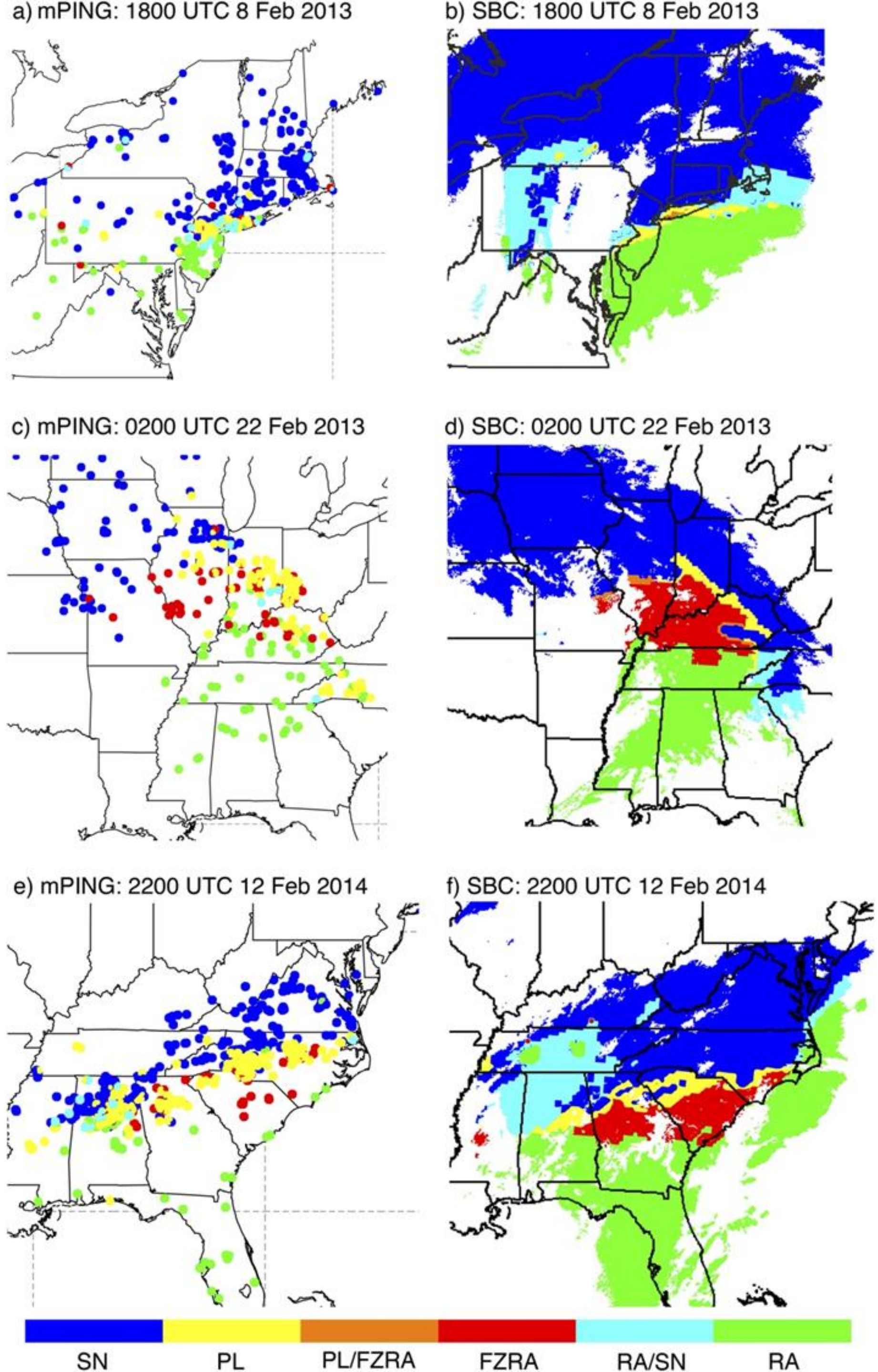
a) mPING: 1800 UTC 8 Feb 2013
b) SBC: 1800 UTC 8 Feb 2013
c) mPING: 0200 UTC 22 Feb 2013
d) SBC: 0200 UTC 22 Feb 2013
e) mPING: 2200 UTC 12 Feb 2014
f) SBC: 2200 UTC 12 Feb 2014
SN
PL
PL/FZRA
FZRA
RA/SN
RA

Columnar vertical profiles (CVP) of polarimetric radar variables through the ML measured during MCS on May 20, 2011

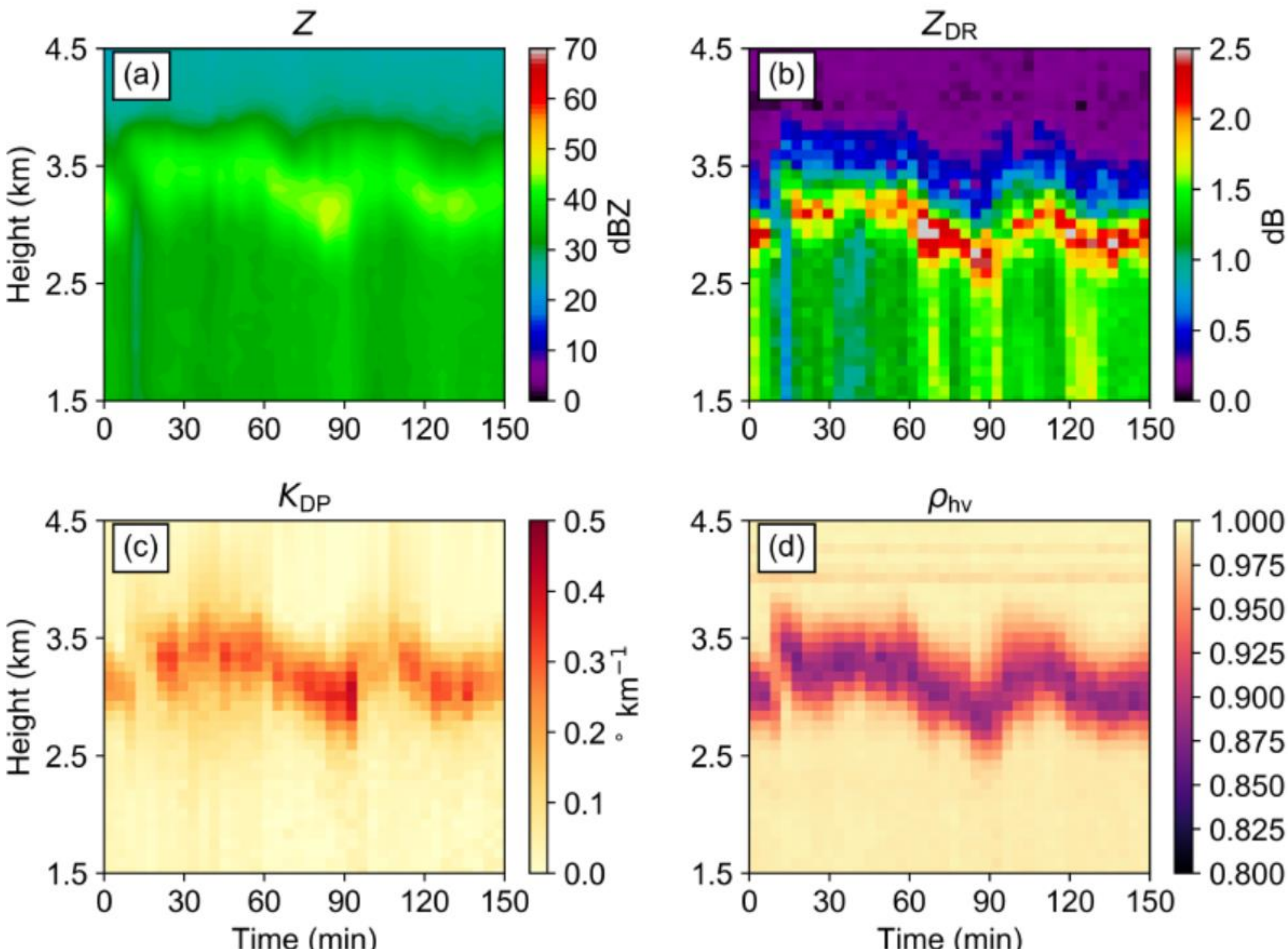

Comparison of simulated and observed vertical profiles of radar variables within the melting layer

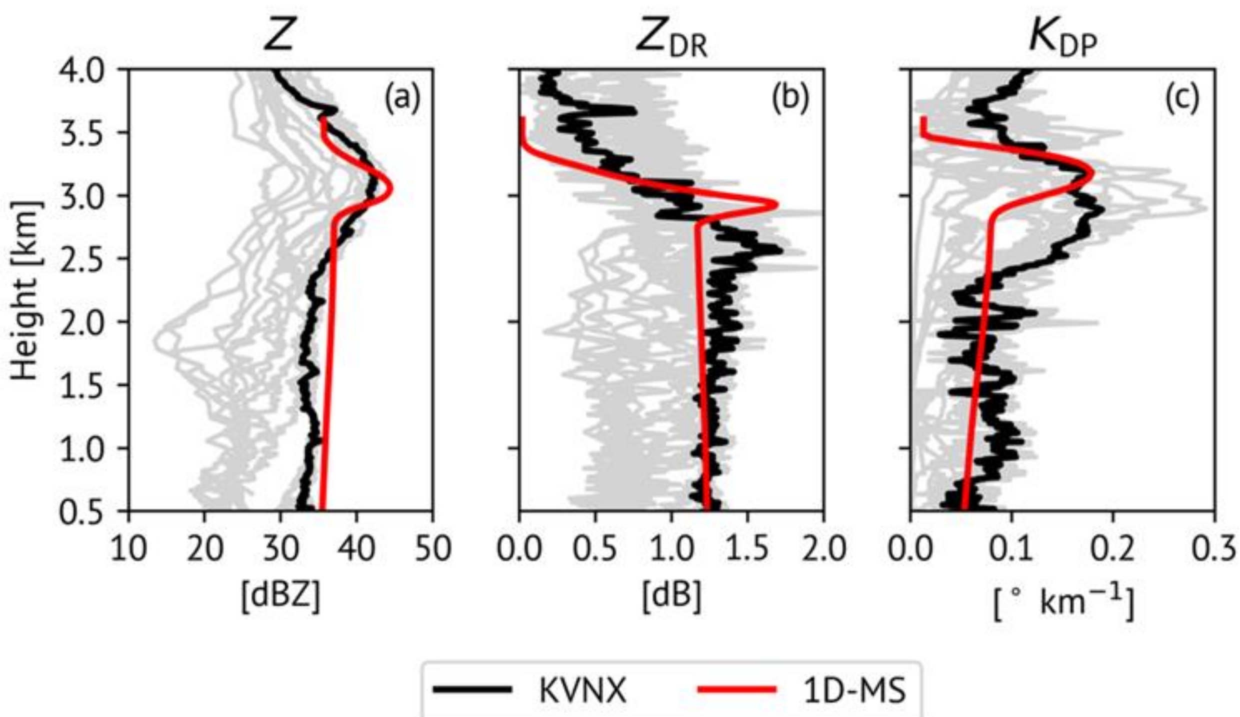

Simulating possible mechanisms causing modulation of the ML height and strength

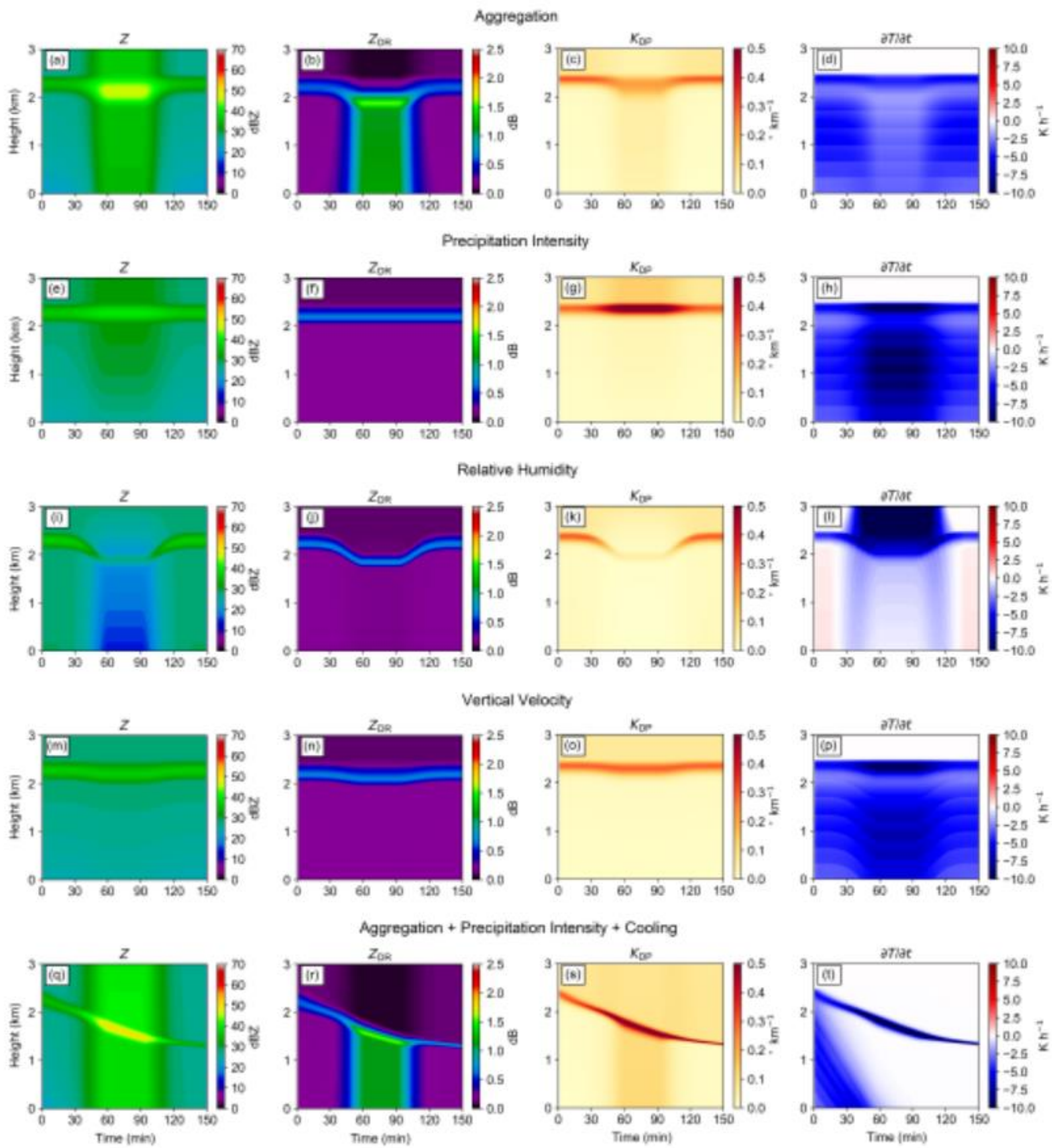

Maximum ***Z*** v. **Cooling Rate** in the Melting Layer

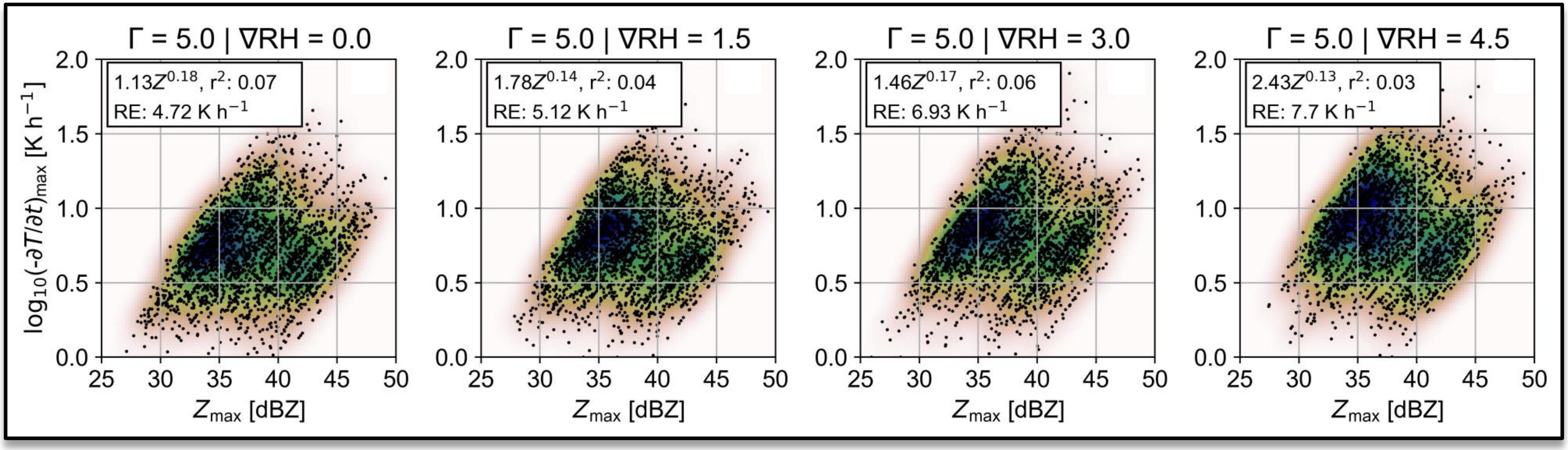

Maximum *Z* in the brightband contains *little to no information* about the maximum cooling rate in the melting layer (high RMSE, low r^2).

Bulk of cooling is due to smallest particles, with *Z* a strong function of the largest particles.

Maximum **Δ*Z*** v. **Cooling Rate** in the Melting Layer

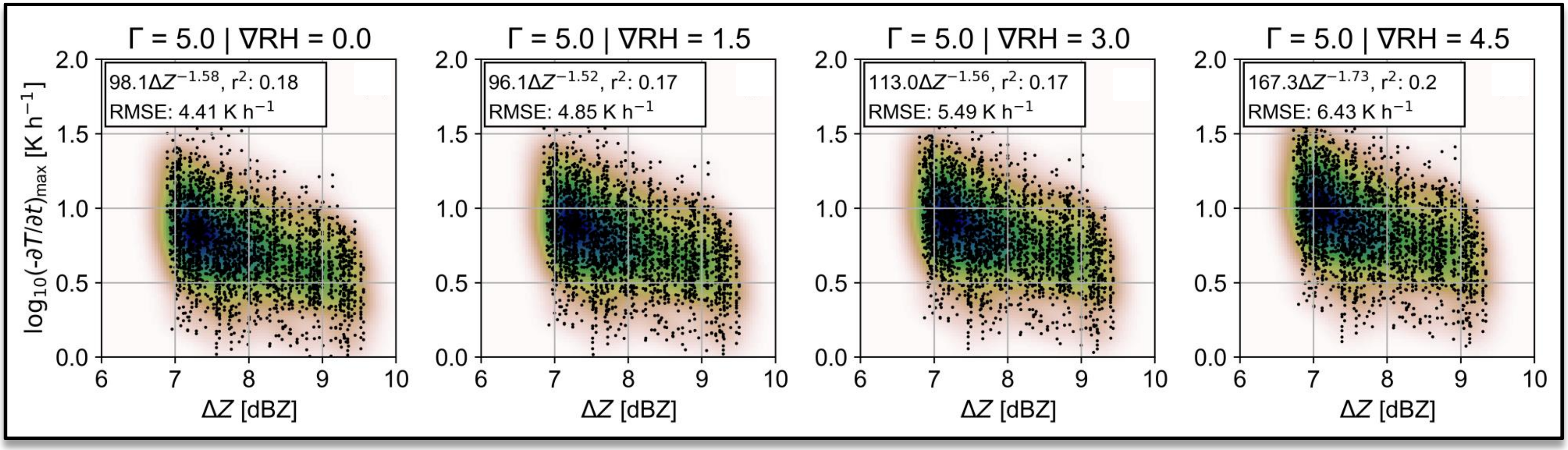

Maximum ΔZ in the brightband tends to decrease for increasing cooling rates as distributions with large numbers of small particles tend to have smaller D_{max}.

Maximum ΔZ in the brightband contains *little to no information* about the maximum cooling rate in the melting layer (high RMSE, low r^2).

Maximum K_{DP} v. **Cooling Rate** in the Melting Layer

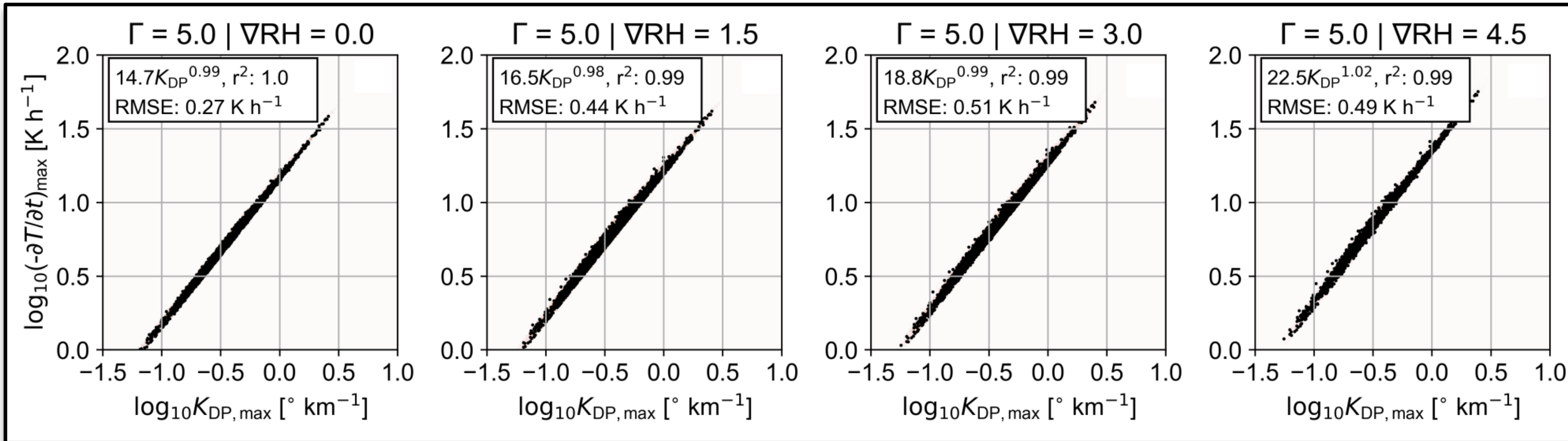

Maximum K_{DP} in the brightband is *very highly correlated* with the maximum cooling rate in the melting layer (low RMSE, high r^2), in stark contrast to all other variables.

Coefficient of linear relationship changes as a $f(\Gamma,RH)$.

What is responsible for this strong $K_{DP,max}$– $\partial T/\partial t_{max}$ relationship?

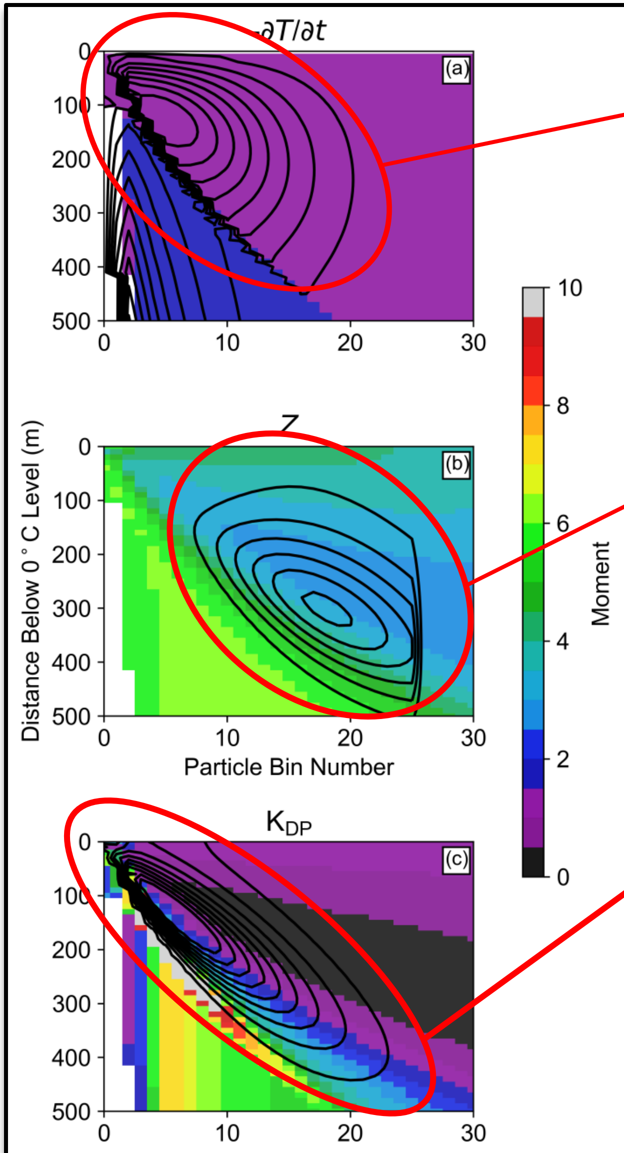

Particle bin number

The cooling rate is approximately proportional to $M_{1.5}$ of the PSD.

Z is approximately proportional to M_3 – $M_{3.5}$ of the PSD.

K_{DP} is approximately proportional to the $M_{1.5}$ of the PSD for the bins with the majority of the contribution to K_{DP}.

Moment of PSD variable ∝ to

Contribution of variable in each bin

Contribution of different processes to cooling rates in hailstorms below the freezing level

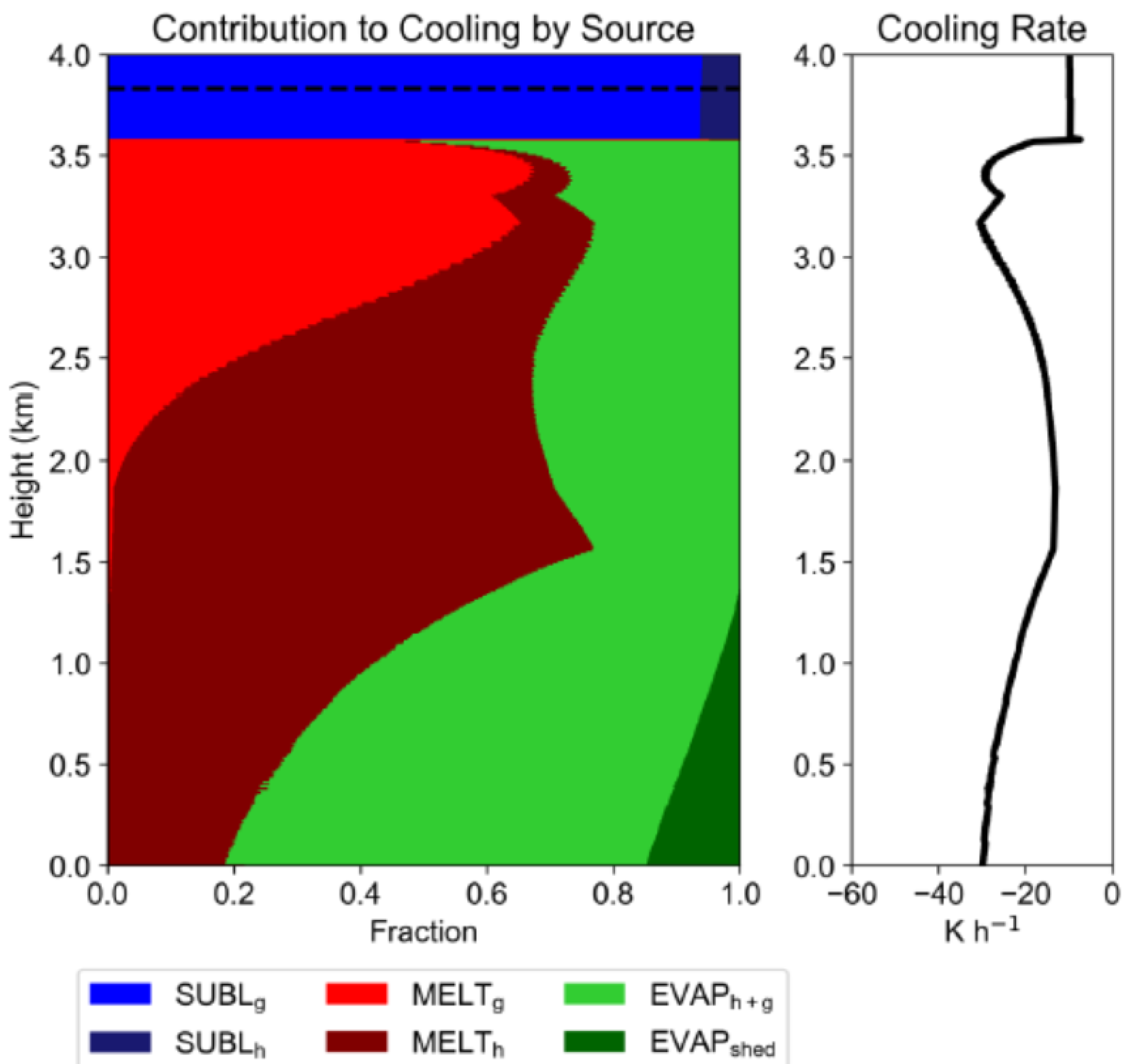

Correlations of maximal cooling rate with various radar variables in hailstorm below the freezing level

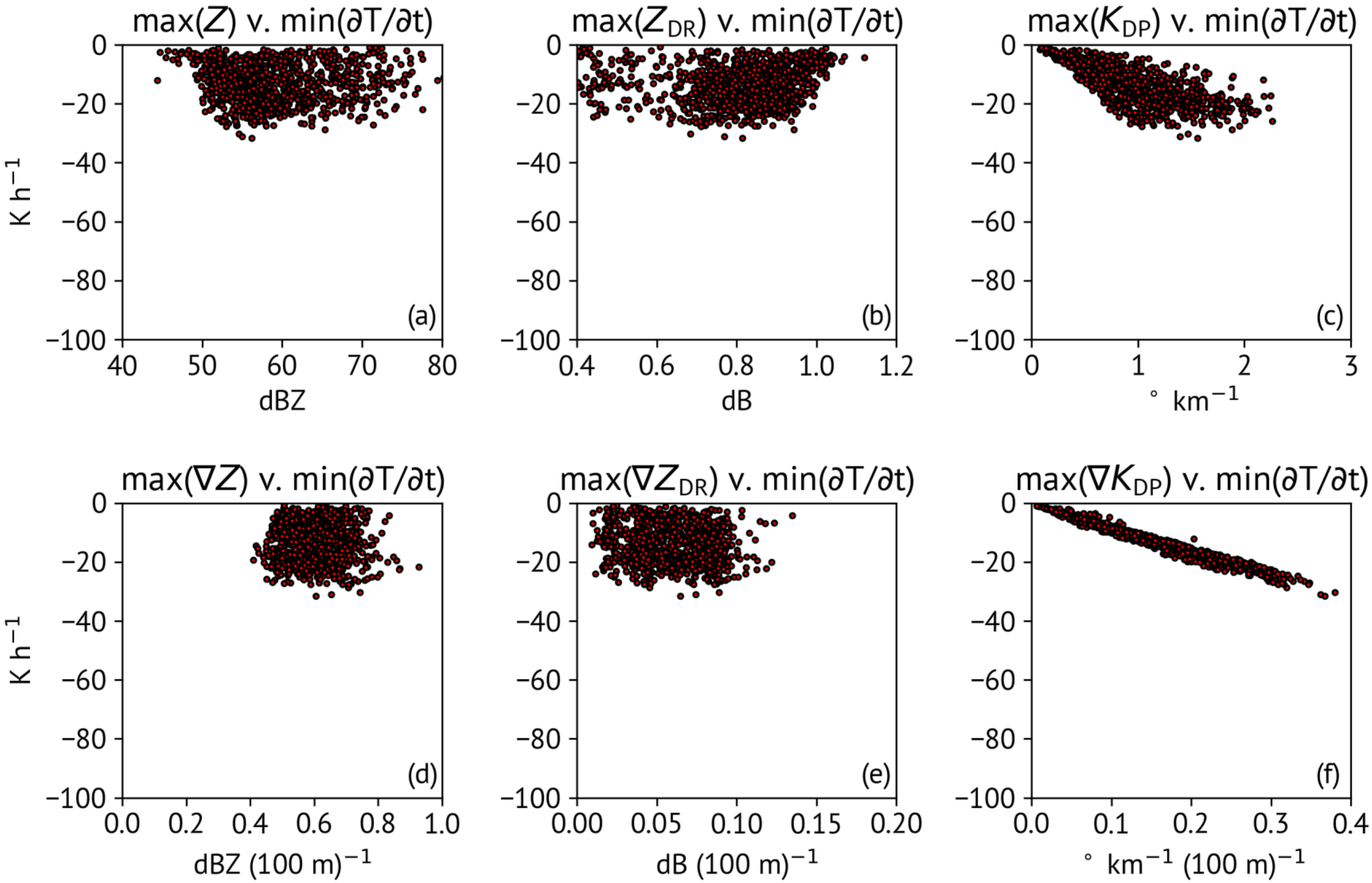

Forward operators

Pfeifer et al. (2008) A poalrimetric radar forward operator for model evaluation

Jung et al. (2008) Assimilation of simulated polarimetric radar data for a convective storm using an Ensemble Kalman Filter, Part I: Observations operators for reflectivity and polarimetric variables

Ryzhkov et al. (2011) Polarimetric radar observation operator for a cloud model with spectral microphysics

Zeng et al. (2016) An efficient modular volume-scanning radar forward operator for NWP models: description and coupling to the COSMO model

Wolfensberger and Berne (2018) From model to radar variables: a new forward polarimetric radar operator for COSMO

Modeling intrinsic and measured vertical profiles of Z, Z_{DR}, and ρ_{hv} within the melting layer

Intrinsic vertical profiles of Z, Z_{DR}, and ρ_{hv}

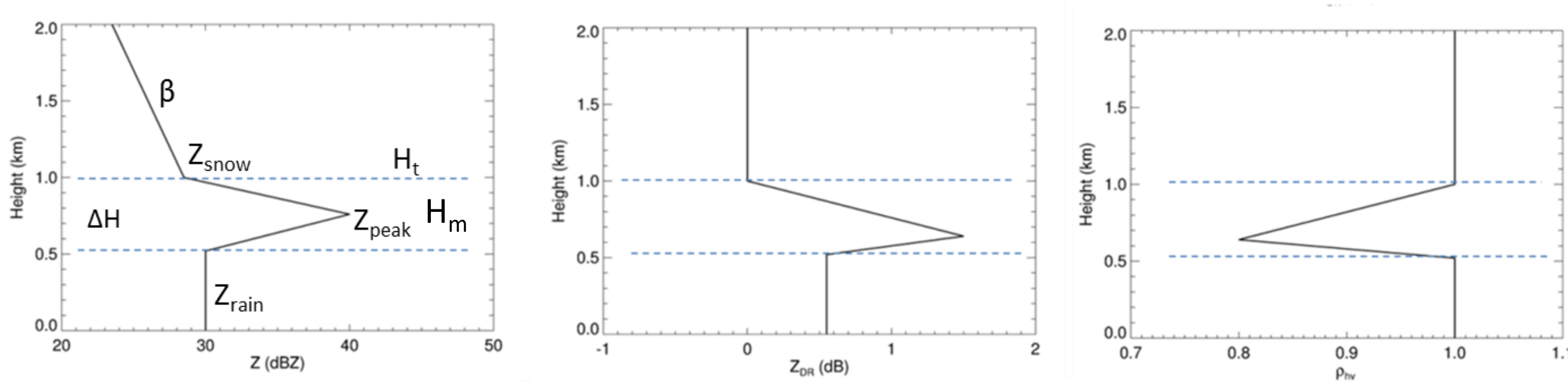

Measured vertical profiles of Z, Z_{DR}, and ρ_{hv} at r = 50 km

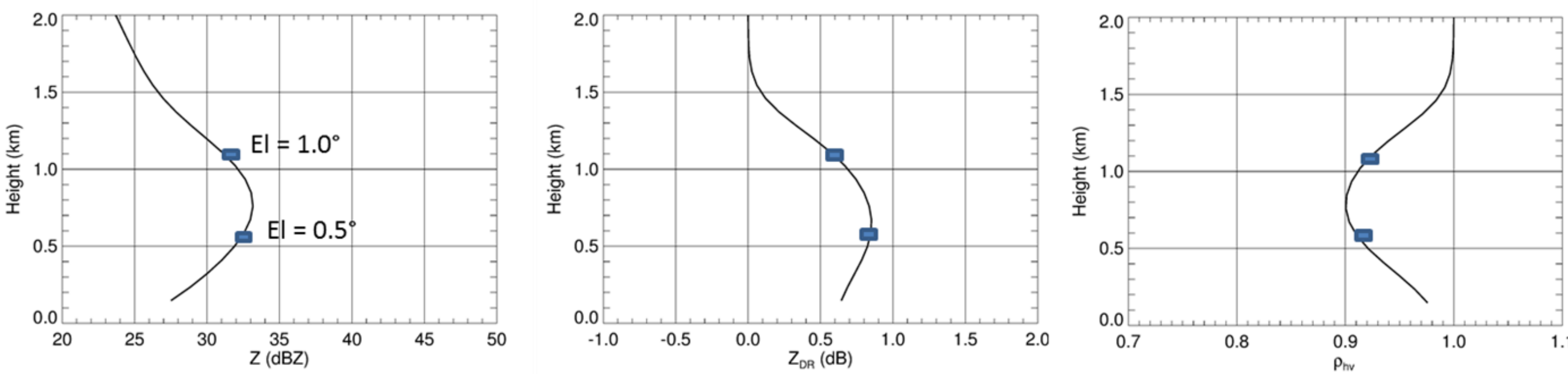

Intrinsic profiles are parameterized by a limited number of parameters: the differences between maximal values of Z and Z_{DR} within the ML and the ones in rain, depth of the ML, slope of the vertical dependence of Z above the ML, etc.

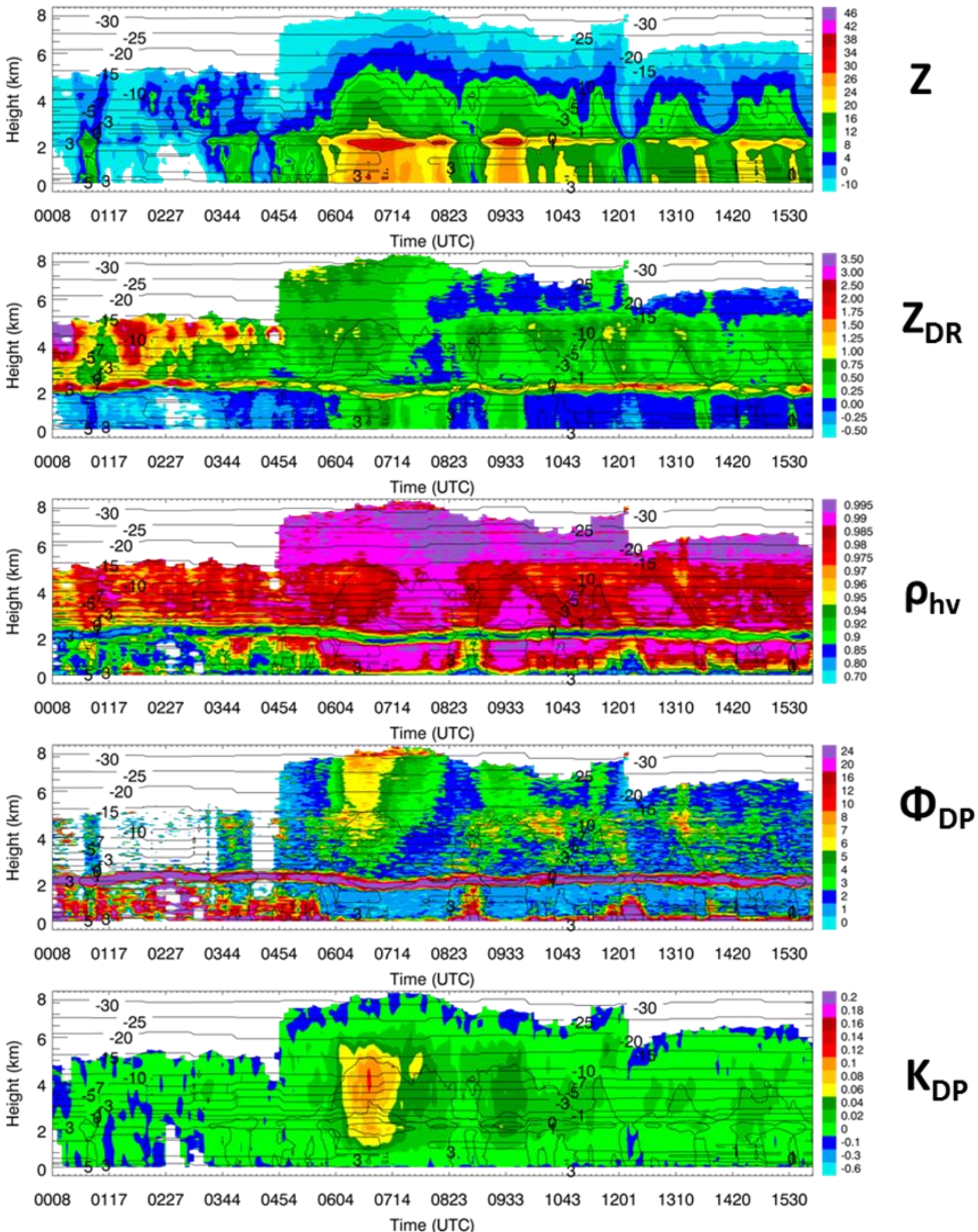
Z
Z_DR
ρ_hv
Φ_DP
K_DP
Height (km)
Time (UTC)
0008 0117 0227 0344 0454 0604 0714 0823 0933 1043 1201 1310 1420 1530

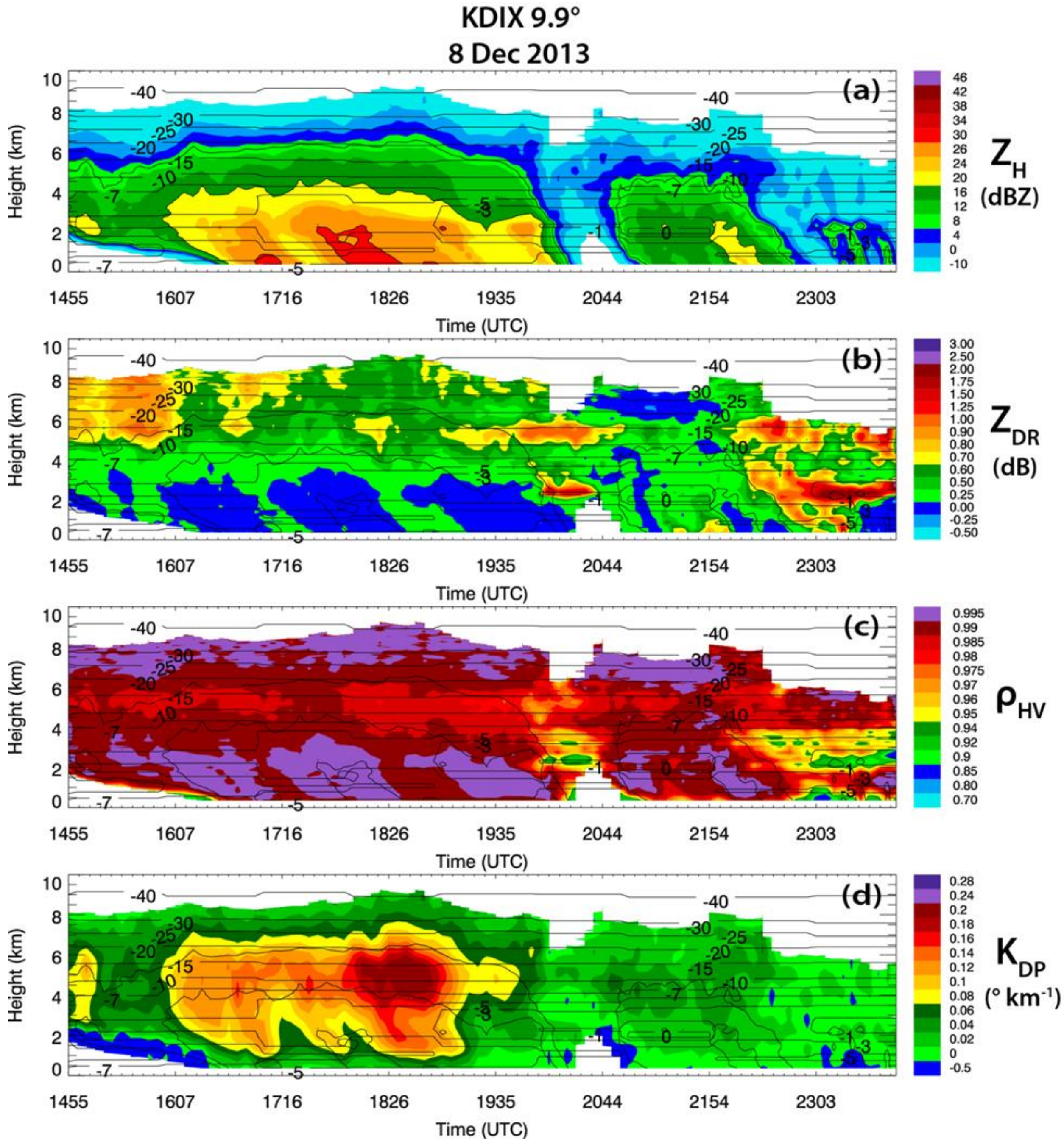

KDIX 9.9°
8 Dec 2013
(a)
(b)
(c)
(d)
Height (km)
Time (UTC)
1455
1607
1716
1826
1935
2044
2154
2303
Z_H (dBZ)
Z_DR (dB)
ρ_HV
K_DP (° km^-1)

QVP within the melting layer at S band

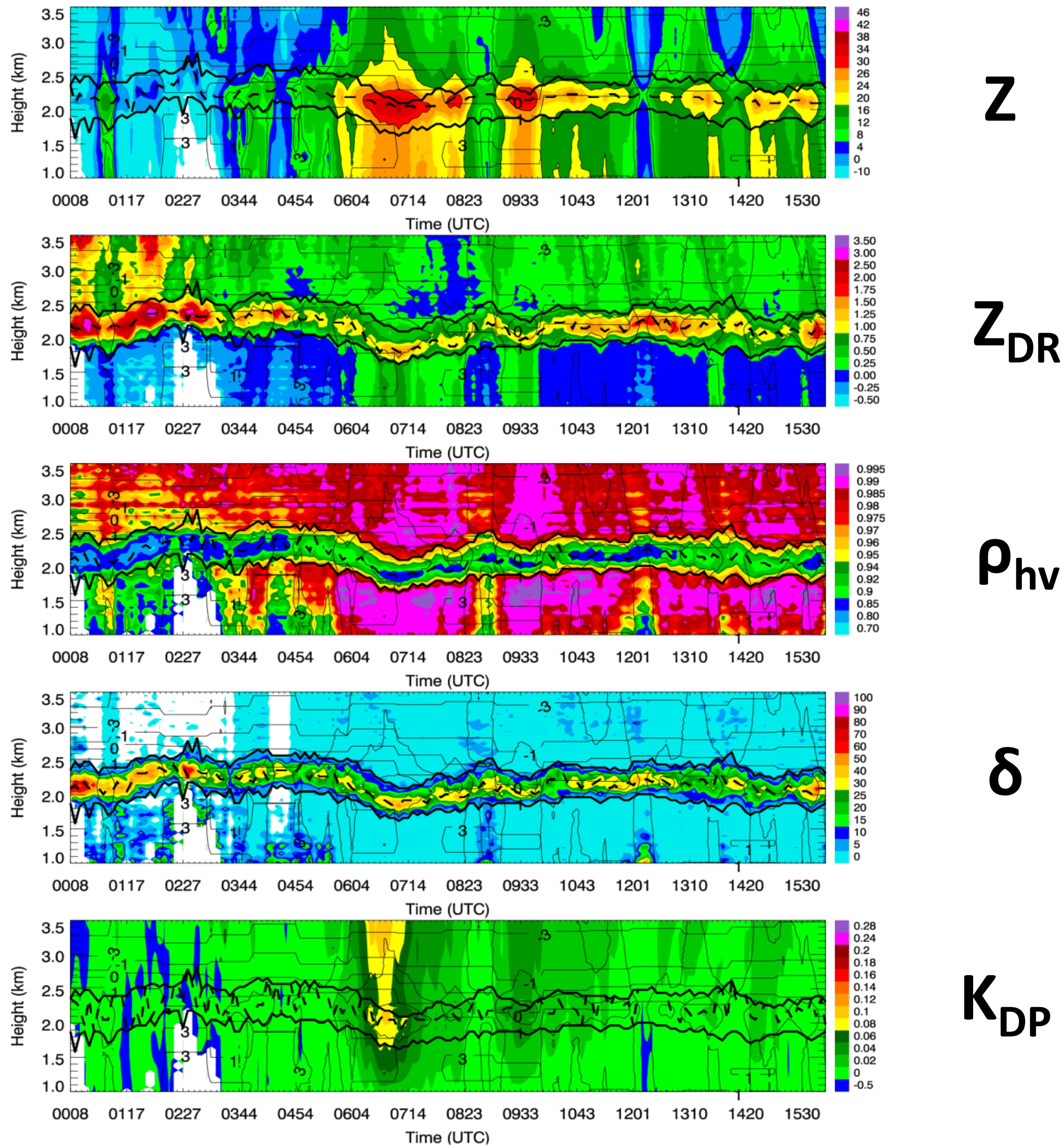

Refreezing signature

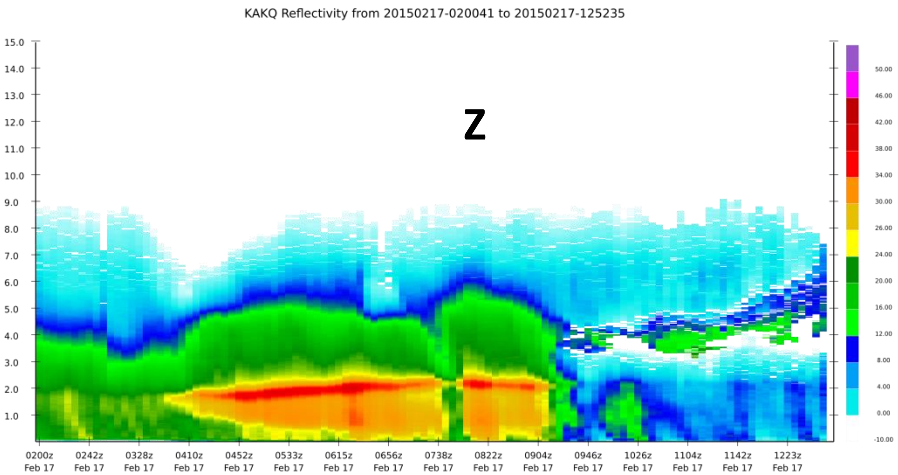

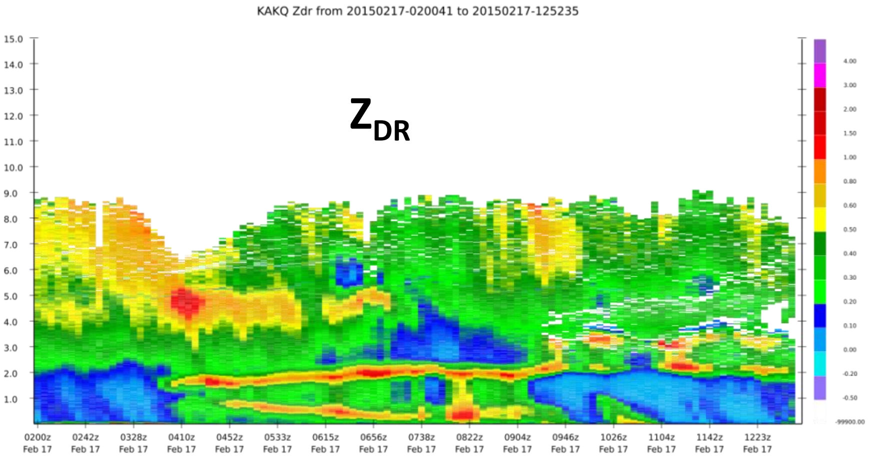

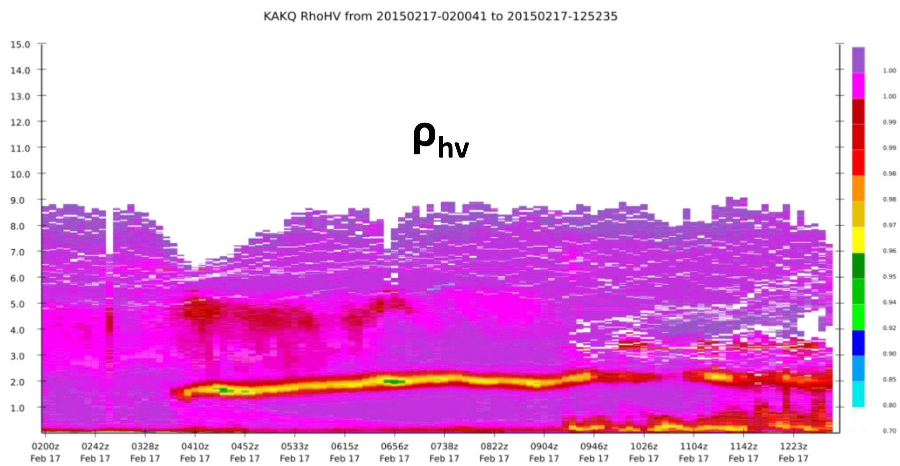

Estimation of the width of the canting angle distributions σ

$$\frac{C_{dr}}{L_{dr}} \approx \frac{<|s_h|^2>}{<|s_h + s_v|^2>} \frac{1}{\sigma^2 + <\alpha>^2}$$

$<\alpha>$ - mean canting angle
σ – width of the canting angle distribution
$s_{h,v}$ – scattering amplitudes at H and V polarizations

$$\sigma^2 = \frac{<|s_h|^2>}{<|s_h + s_v|^2>} \frac{L_{dr}}{C_{dr}} \qquad <\alpha> = 0$$

Linear depolarization ratio Ldr is a function of particle orientations whereas circular depolarization ratio CDR is not

$$C_{dr} \approx \frac{1 + Z_{dr}^{-1} - 2\rho_{hv} Z_{dr}^{-1/2}}{1 + Z_{dr}^{-1} + 2\rho_{hv} Z_{dr}^{-1/2}}$$

Cdr can be approximately estimated from Zdr and ρ_{hv} (Ryzhkov et al. 2017)

$$\frac{<|s_h|^2>}{<|s_h + s_v|^2>} = \frac{1}{1 + Z_{dr}^{-1} + 2\rho_{hv} Z_{dr}^{-1/2}}$$

$$\sigma^2 = \frac{L_{dr}}{1 + Z_{dr}^{-1} - 2\rho_{hv} Z_{dr}^{-1/2}}$$

The width of the canting angle distribution σ can be estimated from the combination of Ldr, Zdr, and ρ_{hv}

$$\sigma(\deg) = \frac{180}{\pi} \frac{L_{dr}^{1/2}}{(1 + Z_{dr}^{-1} - 2\rho_{hv} Z_{dr}^{-1/2})^{1/2}}$$

Ldr and Zdr are expressed in linear scale

QVP SPOL
20111127 00:00-23:59 UTC

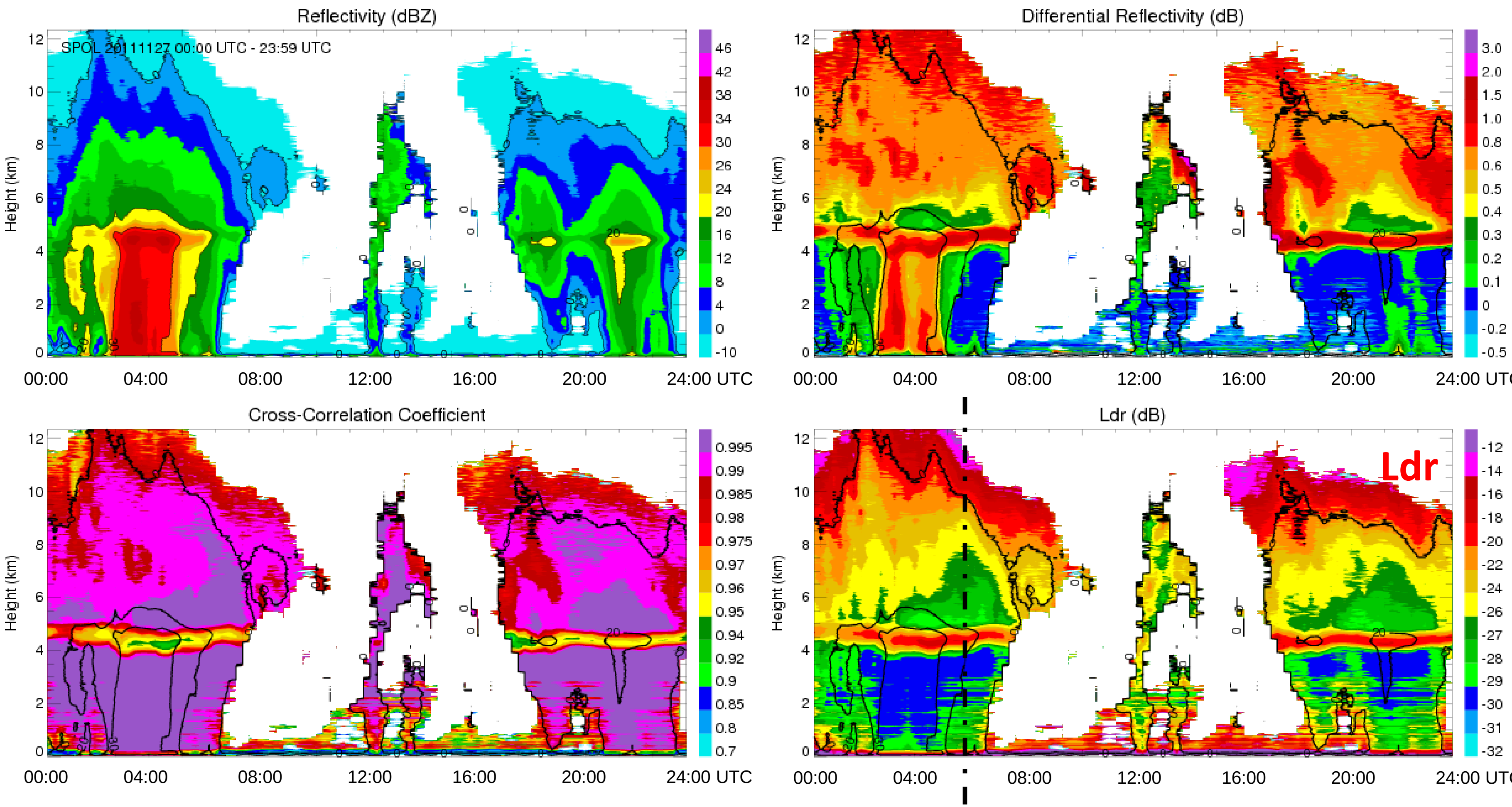

Vertical profiles of Z_{DR} and σ

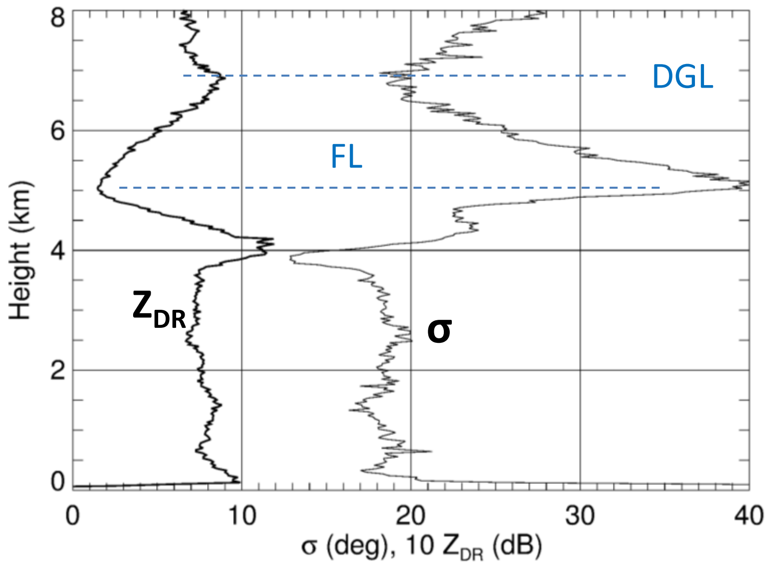

DGL – dendritic growth layer
FL – freezing level

The orientation spread σ is highly variable and may increase by a factor of 2 as a result of snow aggregation.